CFD Modeling of LNG Spill: Humidity Effect on Vapor Dispersion

S G Giannissi[1,2], A G Venetsanos[1] and N Markatos[2]
[1] Environmental Research Laboratory, National Center for Scientific Research Demokritos, Agia Paraskevi 15310, Greece
[2] School of Chemical Engineering, National Technical University of Athens, Heroon Polytechniou 9, Zografou, 15780, Greece

E-mail:sgiannissi@ipta.demokritos.gr

Abstract. The risks entailed by an accidental spill of Liquefied Natural Gas (LNG) should be indentified and evaluated, in order to design measures for prevention and mitigation in LNG terminals. For this purpose, simulations are considered a useful tool to study LNG spills and to understand the mechanisms that influence the vapor dispersion. In the present study, the ADREA-HF CFD code is employed to simulate the TEEX1 experiment. The experiment was carried out at the Brayton Fire Training Field, which is affiliated with the Texas A&M University system and involves LNG release and dispersion over water surface in open-obstructed environment. In the simulation the source was modeled as a two-phase jet enabling the prediction of both the vapor dispersion and the liquid pool spreading. The conservation equations for the mixture are solved along with the mass fraction for natural gas. Due to the low prevailing temperatures during the spill ambient humidity condenses and this might affect the vapor dispersion. This effect was examined in this work by solving an additional conservation equation for the water mass fraction. Two different models were tested: the hydrodynamic equilibrium model which assumes kinetic equilibrium between the phases and the non hydrodynamic equilibrium model, in order to assess the effect of slip velocity on the prediction. The slip velocity is defined as the difference between the liquid phase and the vapor phase and is calculated using the algebraic slip model. Constant droplet diameter of three different sizes and a lognormal distribution of the droplet diameter were applied and the results are discussed and compared with the measurements.

1. Introduction

The use of natural gas as fuel has increased over the past few years and its flammable nature generates the necessity of performing safety assessment, in order to indentify the risks and design measures for prevention and mitigation in case of an accident. A common practice for handling, storage and transportation of natural gas is its liquefaction at low temperatures. Therefore, it is significant to investigate the dispersion of liquefied natural gas (LNG).

A useful tool to investigate the behavior and dispersion of LNG are the CFD codes. Prior to the use of the CFD codes a validation of the code should be carried out, in order to asses its performance. The validation should be performed against several experiments.


Content from this work may be used under the terms of the Creative Commons Attribution 3.0 licence. Any further distribution of this work must maintain attribution to the author(s) and the title of the work, journal citation and DOI.
Published under licence by IOP Publishing Ltd

In the present study the ADREA-HF CFD code [1] is used to simulate the TEEX1 trial of the BFTF experimental series. TEEX1 involves the release and dispersion of LNG over water surface in a confined area [2]. The ADREA-HF code has been validated against other LNG experiments [3], and against the dispersion of others gases [1] and cryogenic fluids [4] and has shown satisfactory agreement with the experiments.

During a LNG release the ambient humidity condenses due to the low prevailing temperatures. The liquid droplets that are formed might develop different velocity than the vapor phase and fall faster to the ground. The difference between the velocity of the liquid and the velocity of the vapor phase is called slip velocity. A non-hydrodynamic equilibrium model which takes into account the slip velocity is employed in the present study. Three different constant droplet diameters (50, 100 and 200 μm) and a lognormal diameter distribution with 50μm mean diameter were considered for the sensitivity study.

The computational results showed that the results with the slip model assuming a 200μm constant diameter or a lognormal distribution with mean diameter 50 μm are in better agreement with the experiment, especially at the higher sensors.

2. Experimental description

Six small and medium tests were performed at the Brayton Fire Training Field (BFTF), Texas A&M University between 2005 and 2009. During these experiments LNG was spilled above water surface with 45-degree angle in a confined area. TEEX1 test (07LNG01) is simulated here. The experimental site is depicted in Figure 1. The pit was filled with water, and 1.3m high wooden boards were erected around the pit as obstacles. 40 gas detector poles were located outside the fence with south east direction to monitor the methane concentration at several heights.



Figure 1. The experimental site [2].

During the TEEX1 the wind direction was varied from south east to south and the average velocity at 2.3 m was 1.2 m. Table 1 summarizes the release and weather conditions for TEEX1.

Table 1. A summary of the release and weather conditions.

Parameter	Value	Parameter	Value
Source diameter (m)	0.063	Pond temperature (K)	293
Spill rate (m^3/min)	0.75	Wind speed (m/s) #1	1.2
Spill duration (sec)	619	Measur. height for wind speed (m) #1	2.3
Fence length (m)	10	Wind speed (m/s) #2	1.9
Fence width (m)	6.4	Measur. height for wind speed (m) #2	10
Fence height (m) - above water surface	1.3	Wind direction (deg)	160
Relative humidity (%)	32.6	Measur. height for wind direction (m)	2.3

Ambient temperature #1 (K)	289.05	Roughness length z0 for water (m)	0.0004
Measur. height for temperature #1 (m)	2.3	Roughness length z0 (m)	0.00085
Ambient temperature #2 (K)	289.05	Friction velocity u-star (m/s)	0.053
Measur. height for temperature #2 (m)	10	Monin-Obukhov length (m)	8.3

3. Modeling set-up

3.1. Mathematical equations

The transient three dimensional mass, momentum and enthalpy conservation equations for the mixture and the mass fraction conservation equation of each component (methane and water) are solved,

$$\frac{\partial \rho}{\partial t}+\frac{\partial \rho u_i}{\partial x_i}=0 \tag{1}$$

$$\frac{\partial \rho u_i}{\partial t}+\frac{\partial \rho u_j u_i}{\partial x_j}=-\frac{\partial p}{\partial x_i}+\frac{\partial}{\partial x_j}\left((\mu+\mu_t)\left(\frac{\partial u_i}{\partial x_j}+\frac{\partial u_j}{\partial x_i}\right)\right)+\rho g_i-\delta_{3i}\frac{\partial}{\partial z}\left(\rho q_\ell w_{sl}(1-q_\ell)w_{sl}\right) \tag{2}$$

$$\frac{\partial \rho q_k}{\partial t}+\frac{\partial \rho u_j q_k}{\partial x_j}=\frac{\partial}{\partial x_j}\left(\left(\rho d+\frac{\mu_t}{Sc_t}\right)\frac{\partial q_k}{\partial x_j}\right)-\frac{\partial \rho w_{sl}\left(q_{\ell_k}-q_k q_\ell\right)}{\partial z} \tag{3}$$

$$\frac{\partial \rho H}{\partial t}+\frac{\partial \rho u_j H}{\partial x_j}=\frac{\partial}{\partial x_j}\left(\frac{\mu_t}{Pr_t}\frac{\partial H}{\partial x_j}\right)+\frac{Dp}{Dt}+\frac{\partial}{\partial z}\left[\rho q_\ell w_{sl}(H-H_\ell)\right]-q_\ell w_{sl}\left(1-\frac{\rho}{\rho_\ell}\right)\frac{\partial p}{\partial z} \tag{4}$$

For the turbulence modeling the standard k-ε model with extra buoyancy terms [1] is used. The last terms in the right side of equations (2), (3) and (4) are activated when the non-hydrodynamic equilibrium model is employed. In the hydrodynamic equilibrium model these terms are zero.

In the above equations ρ is the mixture density (kg/m^3), u is the velocity vector (m/s), P is the pressure (Pa), g is the gravity vector (m/s^2), μ and μ_t are the laminar and turbulent viscosity, respectively (kg/m/s), Pr_t is the dimensionless turbulent Prandtl number, d is the molecular diffusivity of methane to air (m^2/s), Sc_t is the dimensionless turbulent Schmidt number, H is the enthalpy, and q is the mass fraction. Prandtl number and Schmidt number are set equal to 0.72. The subscripts i, j, k denote the Cartesian i, j coordinates and the component k, respectively, the indexes ℓ, v stand for the liquid and vapor phase, respectively, and index sl stands for the slip velocity.

3.2. Initial and inflow weather conditions

Initial and inflow wind profile should be set during the simulation. To derive the velocity profile of the wind and the k, ε values the atmospheric conditions should be taken into account. The velocity, the k and the ε values can be estimated based on the Monin-Obukhov similarity theory. In the present study the Monin-obukhov length is positive and corresponds to stable conditions. The value of Monin-Obukhov length as indicated in Table 1 was used, in order to calculate the wind profile according to the following equations,

$$u(z)=\frac{u_*}{\kappa}\left[\ln\left(\frac{z}{z_0}\right)-\psi_m\left(\frac{z}{L}\right)\right] \tag{6}$$

$$\text{where } \psi_m\left(\frac{z}{L}\right) = -5\frac{z}{L} \tag{7}$$

$$k = 6u_*^2 \tag{8}$$

$$\varepsilon = \frac{u_*}{\kappa z}\left(1.24 + 4.3\frac{z}{L}\right) \tag{9}$$

In [2] it is mentioned that even though a south wind was observed at the early stage of the release as the test proceeded the wind shifted and according to the experimental concentration contours the south east direction seems to be dominant during the experiment. Therefore, a south east direction was assumed during the entire simulation.

3.3. Computational grid

The zero reference point was set on the right, leeward corner (see Figure 2). The computational domain was extended in the y-axis 9.6 m from the windward fence wall and 40m from the leeward fence wall. A symmetry plane was assumed along the x-axis and the computational domain is extended 50 m from the right wall. The domain in the z-axis was extended 6 m. A grid with total number of cells equal to 70576 was used. Refinement was applied near the release point, the fences and the ground.

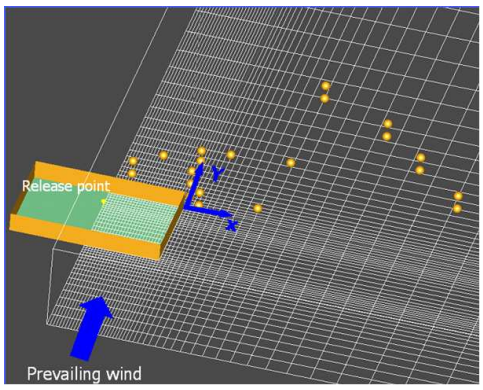


Figure 2. The test site and the computational grid on the bottom. The orange spheres represent the sensors that deployed in the simulation.

3.4. Boundary conditions

Symmetry boundary conditions were applied on symmetry plane. In the outlet boundaries a constant pressure boundary conditions was imposed, except for the north plane were zero gradient boundary condition was applied. For the components' concentration and the temperature either a zero gradient boundary condition was applied if outflow occurs or a given value boundary condition if inflow occurs at all outlet boundaries. At the bottom boundary zero gradient boundary conditions was set for all variable except for temperature. The boundary condition for the temperature inside the confined area (water substrate) was constant value equal to 293 K. The surface roughness for water was set as indicated in Table 1. At bottom boundary outside the confined area a concrete substrate was set with properties $\rho = 2371\ \text{kg/m}^3$, $\lambda = 1.13\ \text{J/m/s/K}$ and $c_p = 880\ \text{J/kg/K}$ and a roughness length equal to $8.5\cdot10^{-4}$. A 1-D transient temperature equation is solved inside the underground. The initial and boundary condition at the bottom boundary of the underground was set equal to 289 K.

3.5. Methane inlet conditions

The LNG was released into the pit with 45-degree angle. However, the exact elevation of the pipeline exit is not available. Based on the photograph of the experimental site (Figure 1) a height of approximately 30cm was assumed. Pure methane was assumed as natural gas and the source was modeled as a two-phase jet. A small fraction of the LNG was flashed vaporized in the pipeline, therefore, a small vapor fraction of 5% v/v was assumed at the source. Due to lack of detailed information this fraction is not certain. However, a sensitivity study with 10 and 15 % v/v flash fractions showed little effect on the results.
The measured volumetric flow rate was equal to 0.75 m^3/min. Using the liquid density the mass flow rate is estimated. The velocity at the source was estimated using the mass flow rate and the mixture density, which was calculated with the help of the flashed vapor volume fractions.

3.6. Slip model
In the presence of humidity in the atmosphere the water condenses and freezes since the prevailing temperatures (near the release point the temperature is 111.5 K) are below the water boiling point. The humidity phase change liberates heat and the cloud becomes more buoyant. The droplets that are formed can develop different velocities and might fall faster to the ground. The difference between the phases' velocity is called slip velocity.
The slip velocity is derived by,

$$w_{sl} = \frac{1}{18\mu f_{drag}}\left(\rho_\ell - \rho\right) g D^2 \tag{10}$$

To model this phenomenon a non hydrodynamic equilibrium model should be employed, which allows the phases to obtain different velocities.
According to the diameter size the flow regime can be laminar, transition or turbulent. The drag function, f_{drag}, defines the flow regime, and its value is given by [5]:

$$f_{drag} = \begin{cases} 1+0.15 Re_p^{\,0.687}, & Re_p \le 1000 \\ 0.01833 Re_p, & Re_p > 1000 \end{cases} \tag{11}$$

As humidity condenses a cloud droplet of small size, approximately 20μm is formed. The cloud droplets are so small that they are considered to follow the mean flow. Then, as more water condenses, two or more droplets collide and coalescence to form larger droplets. The larger droplets may develop different velocities due the gravitational acceleration. The droplet diameter is an unknown parameter; therefore, a sensitivity study was performed assuming a constant diameter of 50, 100 and 200μm. Furthermore, a model that assumes a lognormal droplet diameter distribution was developed and used in the present study,

$$n(D) = \frac{n_0}{D\tilde{\sigma}\sqrt{2\pi}} \exp\left(-\frac{\left(\ln D/\tilde{D}\right)^2}{2\tilde{\sigma}^2} \right) \quad \gamma\iota\alpha\ D>0 \tag{12}$$

The unknown parameters are the parameters $\tilde{D}$ and $\tilde{\sigma}$ and the total number of droplets, n_0. The dimensionless parameter $\tilde{\sigma}$ is given by,

$$\tilde{\sigma} = \ln(\sigma), \quad \sigma \in (1.5, 2.5) \tag{13}$$

A value of σ=2.0 was used here and a mean diameter of 50μm was assumed. The total number of droplets can be estimated by the mean diameter and the liquid mass fraction using the following relationship,

$$n_0 = \frac{6\rho q_\ell}{\rho_\ell \pi \bar{D}^3 \exp\left(3\tilde{\sigma}^2\right)} \tag{14}$$

Finally, in the case with the lognormal diameter distribution the slip velocity is estimated by solving numerically the following integral in order to account for all the flow regimes based on the diameter size,

$$\rho q_{\ell} w_{sl} = \int_0^{\infty} N(D) \rho_{\ell} \frac{\pi}{6} D^3 w_{sl} dD \qquad (15)$$

4. Results and discussion

Figure 3 compares the predictions using the hydrodynamic equilibrium model (no slip model) and the non-hydrodynamic equilibrium model (slip model) with the different droplet sizes with the experiment. Each figure corresponds to a different sensor.

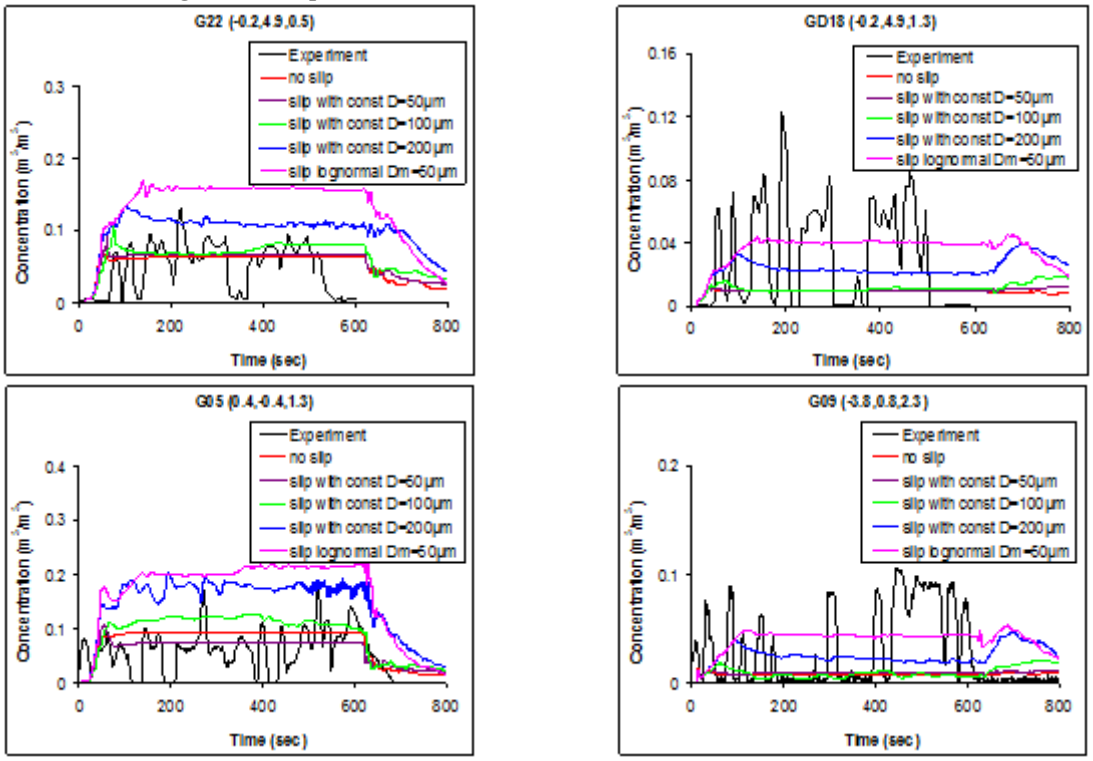


Figure 3. Methane concentration (by volume) time series compared against the experimental data.

The concentration with the hydrodynamic equilibrium model and with the slip model assuming 50μm or 100μm constant droplet diameter is under-predicted at most of the sensors. Assuming diameter of 200μm or lognormal diameter distribution (with mean diameter of 50μm) the predictions are improved and are in better agreement with the experiment at most of the sensors. At the higher sensors the predicted concentration is increased and it is closer to the measurements. This is attributed to the fact that with the slip model the heavy droplets are allowed to obtain different velocity and to fall faster to the ground, leaving a lighter cloud with positive buoyancy. In general, the predictions with the slip model assuming diameter of 200μm or assuming diameter that follows lognormal distribution fall into the range of concentration fluctuations and give less under-prediction of the peak values compared to the no slip model or the slip model assuming small droplet diameters at the higher sensors. The fluctuations in the measurements are due to the turbulence in the wind and they are not reproduced by the simulation. At the low height (0.5m) the simulation results with the slip model and the large diameter (or the lognormal diameter distribution) over-predict reasonably the concentration. This behavior is desirable for determination of the safety zones.

Figure 4 illustrates the predicted concentration contours at 0.5m height using no slip model and the slip model with lognormal diameter distribution. According to the figure the slip model predicts a

narrower cloud and a less extended Lower Flammability Limit (LFL) distance. This is attributed to the fact that a more buoyant cloud is predicted and the dense gas behavior is limited.

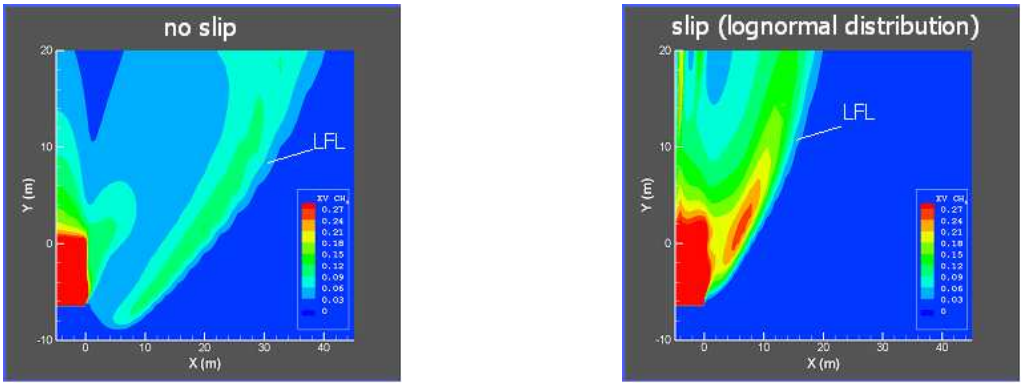


Figure 4. The predicted methane concentration contours at 0.5m height without slip model (left) and with slip model and assuming lognormal diameter distribution (right).

5. Conclusions

In the present study, the spill of liquefied natural gas (LNG) in open-obstructed environment was modeled using the ADREA-HF CFD code. The effect of ambient humidity and its condensation on the vapor dispersion was studied. Humidity condenses and liberates heat. The droplets that are formed by the humidity condensation develop different velocity from the vapor phase, fall faster to the ground and leave a lighter, more buoyant cloud. To model this phenomenon a non-hydrodynamic equilibrium model (slip model) should be employed.

A droplet size parameterization was performed assuming constant diameter of 50, 100 and 200 μm and a lognormal distribution with mean diameter 50 μm. It is shown that the results with a constant diameter of 200μm or assuming lognormal distribution are closer to the measurements compared to the smaller diameters assumption and the no slip model prediction, especially at the higher heights. They tend to slightly over-predict the concentration at the lower heights, which is desirable for determination of the safety zones. However, they still under-predict the peak concentrations at the higher sensors. The predictions assuming smaller diameter and the no slip model underestimate the peak concentrations at all sensors.

Finally, according to the contours figures the simulation without slip model predicts a wider cloud influenced by the dense gas behavior and larger LFL distance crosswind the relase.

6. References

[1] Venetsanos A G, Papanikolaou E and Bartzis J G 2010 *Int. J. Hydrogen Energy* **35** pp. 3908

[2] Cormier B. R., Qi R, Yun G, Zhang Y and Mannan M S 2009 *J. Loss Prev. Process Ind.* **22** 332

[3] Giannissi S G, Venetsanos A G, Markatos N and Bartzis j G 2013 *J. Loss Prev. Process Ind.* **26** 245

[4] Giannissi S G, Venetsanos A G, Markatos N and Bartzis j G 2014 *Int. J. Hydrogen Energy* **39** 15851

[5] L.Schiller and Z.Naumann, 1935 *Z. Ver. Deutsch. Ing.* 77:318